Modification of CdS surface by deposition and annealing of a metal structured organic coating

© S.V. Stetsyura[1], P.G. Kharitonova[1], A.V. Kozlowski[2]

[1] Saratov National Research State University,
410012 Saratov, Russia
[2] Peter the Great St. Petersburg Polytechnical University,
195251 St. Petersburg, Russia

E-mail: haritonovapg@gmail.com

Received May 5, 2025
Revised June 18, 2025
Accepted June 22, 2025

To study the modification of the cadmium sulfide plate surface during deposition and annealing of an iron arachinate coating, we used atomic force microscopy in the amplitude modulation mode to obtain images of the surface relief, distributions of feedback circuit mismatch signals, and phase contrast. It was shown that the combined use of atomic force microscopy oscillatory techniques allowed us to characterize all stages of the creation of the diluted semimagnetic semiconductor material CdS : Fe. New features of the studied surfaces were also discovered by analyzing the statistical parameters obtained from images of atomic force microscopy.

Keywords: atomic force microscopy, cadmium sulfide, iron arachinate, surface modification.

DOI: 10.61011/SC.2025.04.61715.8036

1. Introduction

Creating multicomponent materials with enhanced functionality is one of the modern applied research trends. By modifying the previously known materials and creating heterophase and hybrid structures on basis thereof, not only basic properties may be modified, but also materials and structures controlled by a set of external impacts may be created [1,2]. In this regard, cadmium sulfide (CdS), which is known by its high photosensitivity and doping of which by various atoms may be used to form structures with enhanced functionality, is a promising material [3–5]. Our investigations [6,7] showed that heterophase magnetosensitive structures might be created by introducing Fe atoms into CdS in amounts exceeding the solubility limit of these components.

Unlike other similar techniques [8–10], our technique for fabricating a photosensitive CdS material with FeS phase nanoinclusions involves hybrid structure formation stages, i.e. ultrathin organic iron arachinate (ArchFe) coating on the surface of a single-crystal wafer or polycrystalline CdS films, followed by long-term annealing of the resulting CdS/ArchFe structure in air to undergo Fe atom diffusion, FeS precipitate formation and growth processes, etc. [11]. ArchFe film formation processes and conditions are described in [11]. Monolayer from the surface of a water sub-phase containing 10^{-3} mol/L of $FeCl_3$ was transferred onto the substrate using the Langmuir – Schaeffer method. According to the experiments where all relevant process variables were varied successively, solution pH was set to 4.2 ± 0.05 because it provided formation of the organic ArchFe film without formation of polynuclear hydrocomplexes and large Fe clusters [11]. In these ArchFe monolayer formation conditions, the surface density of Fe atoms in the ArchFe monolayer transferred to a hard substrate reached $N_s = 3.125 \cdot 10^{14}\,\mathrm{cm}^{-2}$, the number of monolayers to be transferred was brought to 25 to increase the specific concentration of Fe atoms in organic coating.

After annealing of the CdS/ArchFe hybrid structure, chemical and phase compositions, and surface topology change because Fe atoms diffuse from the organic ArchFe layer into the CdS film and form a $Cd_xFe_{1-x}S$ solid solution, organic component evaporates because the annealing temperatures exceed the arachic acid sublimation temperature. Due to the limited solubility of Fe and FeS in CdS, several processes were competing: precipitation of new phases, Fe diffusion and surface oxidation, leading to formation of several types of phases arranged unevenly on the surface. The resulting materials have not only a heterophase nanostructure, but also new interesting characteristics, for example, besides an increase in visible light photosensitivity [12], magnetic properties with values typical of diluted magnetic semiconductor materials are observed [13]. Energy-dispersive analysis, Auger spectroscopy and secondary ion mass spectrometry methods were used to detect the $Cd_xFe_{1-x}S$ solid solution formed during Fe diffusion and dissolution in CdS, and nanoscale FeS and Fe_2O_3 phases, due to which the material exhibited the properties of a semimagnetic semiconductor, i.e. of a material combining the properties of conventional and magnetic semiconductors [6]. For brevity, the resulting heterophase material will be denoted as CdS-FeS, indicating only the prevailing and more significant phases.

Multiple experiments showed that the quality and repeatability of this technique depend to a great extent on distribution evenness and organic ArchFe coating uniformity, and potential ArchFe molecule self-organization and

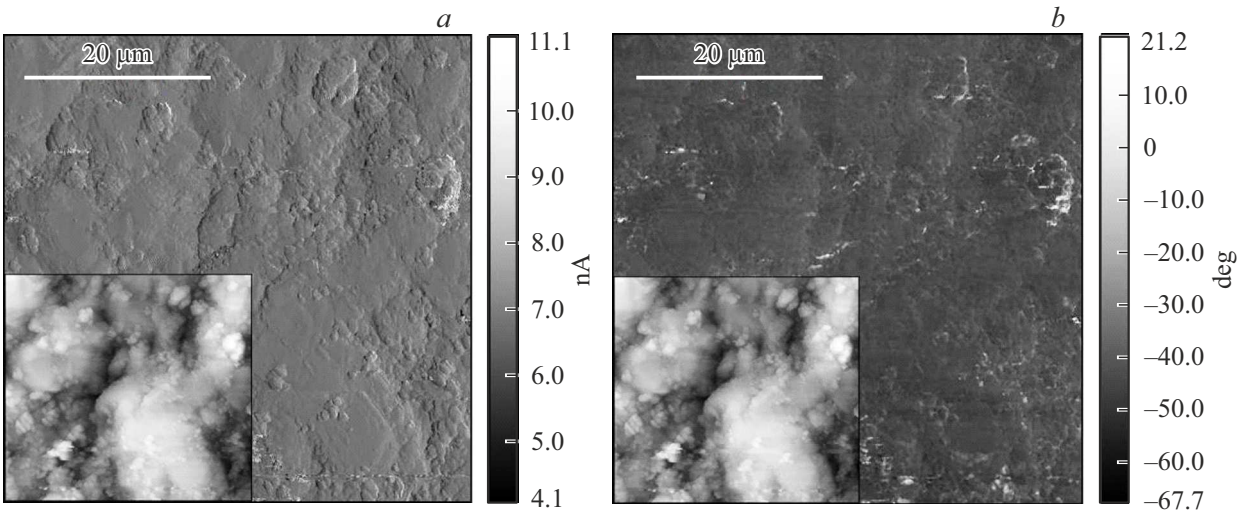

Figure 1. AFM images of „pure“ CdS surface recorded using: *a* — feedback circuit mismatch signal; *b* — phase shift detection methods. Insets — basic AFM image recorded in semicontact surface texture scanning mode.

Fe clustering processes on the CdS surface during annealing. This work provides the results of investigation and combined analysis of atomic force microscopy (AFM) scans of surfaces, including the images of „pure“ CdS (Figure 1), hybrid CdS/ArchFe structure immediately after deposition of the organic coating (Figure 2) and CdS-FeS heterophase material after annealing of the structure in air during 1 hour at 550 °C (Figure 3). Analysis of surfaces at these process stages makes it possible to more fully control formation of diluted magnetic semiconductor materials based on CdS and FeS. Note that surface „status“ changes at each stage — from a potentially uniform semiconductor surface at the first stage to a hybrid surface at the second stage, combining organic, metal-containing and semiconductor components. At the last stage, the surface transforms into a heterophase inorganic one, but possible organic coating residues shall be monitored. Atomic force microscopy (AFM), that allows various signals to be detected during scanning and processed together, ideally fits these tasks.

AFM images were recorded using the INTEGRA SPECTRA AFM microscope (NT-MDT Spectrum Instruments, Russia). Scanning was performed in a semi-contact mode using the FMG01/Pt platinum-coated cantilever. Size of each scan was $50 \times 50\,\mu$m, resolution was 512×512 pixels. Data processing was performed using Gwyddion 2.62 software. AFM image analysis included statistical processing of scans taking into account feedback circuit mismatch (FBCM) signal and phase contrast (phase shift (PS), which reflects the essence of the method more correctly) data, that provides additional information concerning the studied surface when analyzed together with the „basic“ surface texture scan obtained through recording the cantilever oscillation amplitude (in μm or nm).

Thus, the FBCM signal, that is induced by current change inertia in some sensor segments during scanning and is measured in nanoamperes (nA), contains additional information emphasizing small-size surface texture details due to additional consideration of mechanical properties of small surface details, for example, local variations of elasticity forces [14]. The FBCM method is used to monitor small details against relatively large irregularities, and small heterogeneities turn out to be more contrast than large ones due to specific aspects of signal recording. The FBCM method is used to more fully reproduce the texture, in particular on organic coatings and bioobjects [15,16].

Phase shift (PS) signal induced by the phase shift between the incident and reflected beams during scanning and measured in degrees is one of the most widely used AFM visualization methods to detect surface areas that differ in their chemical and mechanical properties such as adhesion, hardness, elasticity and viscosity [17]. Hence, the method is quite promising for investigating hybrid and heterophase materials such as structures combining several components based on polymers and inorganic materials.

Each of Figures 1 to 3 shows a series of images of the same surface area consisting of an AFM image of the basic scan recorded in the semi-contact surface texture scanning mode, and of AFM images recorded using FBCM and PS signal recording and logging methods. Thus, a series of three AFM images characterizing the same surface area is provided for each surface area. Figure 1 shows all above-mentioned AFM images for „pure“ CdS, Figure 2 shows all AFM images for CdS/ArchFe hybrid structure surface, and Figure 3 shows AFM images for the CdS-FeS heterophase surface. The study involves scanning of 8 areas for each samples before and after the modification, Figures 1 to 3 show the same areas of the CdS sample before and after the modification for correct comparison. Gwyddion was used to plot data distributions (heights, nanoamperes, degrees, depending on the type of signal recording) and to determine

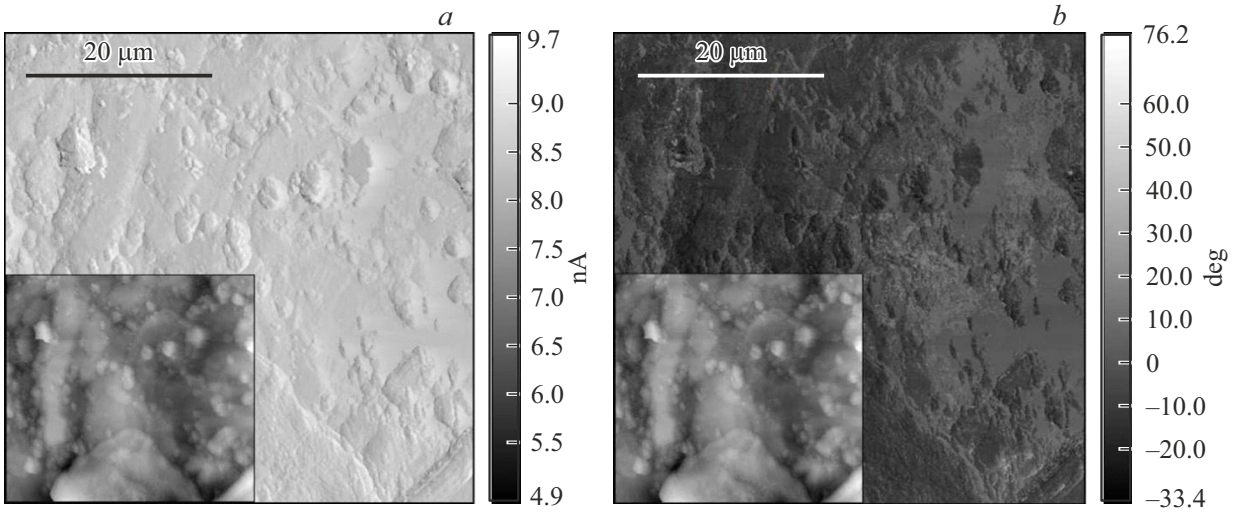

Figure 2. AFM images of the hybrid CdS/ArchFe surface recorded using: *a* — feedback circuit mismatch signal; *b* — phase shift detection methods. Insets — basic AFM image recorded in semi-contact surface texture scanning mode.

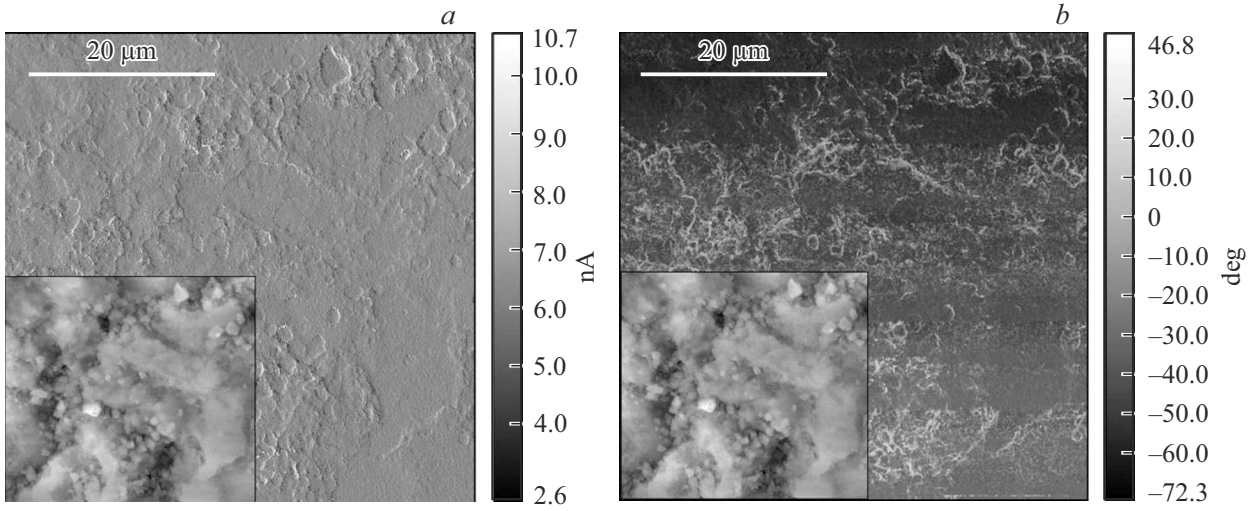

Figure 3. AFM images of the heterophase CdS-FeS surface recorded using: *a* — feedback circuit mismatch signal; *b* — phase shift detection methods. Insets — basic AFM image recorded in semi-contact surface texture scanning mode.

basic statistical parameters, that may be divided into measures of position (characterizing the central distribution tendency), measures of scattering (characterizing the scatter of numerical values with respect to position measures) and measures of shape (characterizing the deviations of experimental distributions from theoretical ones, in this case from the Gaussian distribution). The first group of parameters listed in the table includes an average value and median, the second group includes the average and RMS roughness S_q, and scatter. The third group of parameters (asymmetry γ_1 and excess kurtosis γ_2) is most rarely used for AFM image analysis, but they adequately characterize nonuniform surfaces. Variations of the average and RMS roughnesses are compared most often and were analyzed in detail using the diagrams in Figure 4, that show relative variations of these parameters, while the negative values indicate that the analyzed parameter decreases at the next process stage compared with the previous stage.

Analysis of the „basic“ scans shown in the insets in Figures 1–3 and of the parameters listed in the table for surface texture does not allow one to see their significant differences. In the diagrams in Figure 4, *a*, the average value obtained by surface texture recording increases negligibly when the ArchFe coating is deposited and after annealing (Figure 4, *a*). RMS roughness (dispersion) slightly decreases in transition from the first process stage to the last one (Figure 4, *b*). This may be indirectly indicative of uniform deposition of the ArchFe layer, thickness of which

Statistical parameters characterizing signal distributions for AFM images shown in Figure 1–3

Signal type	Statistical parameter	CdS	CdS/ArchFe	CdS-FeS
Surface texture	Average value, μm	1.5917	1.7004	2.1143
	Median, μm	1.5633	1.6762	2.1764
	RMS roughness (S_q), nm	535.09	489.61	525.76
	Average roughness (S_a), nm	445.72	395.76	422.96
	Scatter (S_z), μm	3.4767	3.9374	4.4221
	Asymmetry (γ_1)	0.0351	0.2067	−0.4211
	Excess kurtosis (γ_2)	−0.7269	0.1531	0.0794
Feedback circuit mismatch	Average value, nA	6.7777	8.3104	6.5794
	Median, nA	6.7730	8.3192	6.7784
	RMS roughness (Sq), pA	374.25	314.82	271.65
	Average roughness (Sa), pA	247.81	222.53	267.03
	Scatter (Sz), nA	6.5568	4.9511	0.6207
	Asymmetry (γ_1)	0.8073	−0.6626	0.0858
	Excess kurtosis (γ_2)	8.1784	3.2302	−1.8688
Phase shift	Average value, degrees	−41.8029	−6.086	−28.2458
	Median, degrees	−42.9641	−7.041	−29.5092
	RMS roughness (S_q), degrees	5.81	7.58	2.51
	Average roughness (S_a), degrees	3.77	6.39	2.15
	Scatter (S_z), degrees	85.4045	109.483	6.7057
	Asymmetry (γ_1)	3.0978	0.3004	1.1078
	Excess kurtosis (γ_2)	16.9649	−0.3757	−0.6755

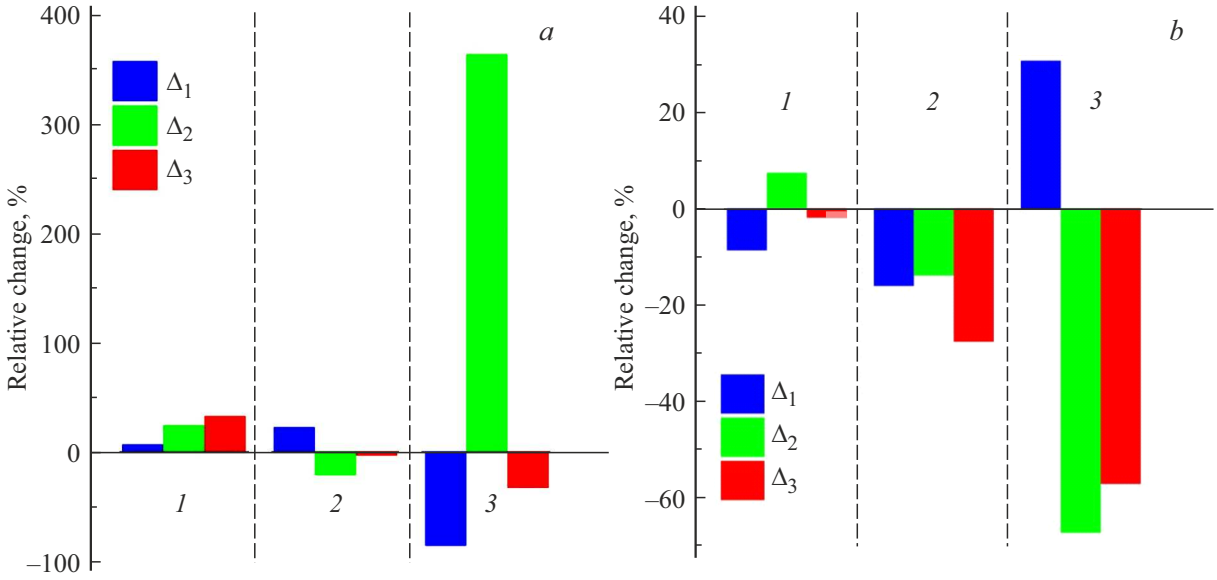

Figure 4. Relative variations of the average roughness (a) and RMS roughness S_q (b) of the surface using three AFM signal recording methods (*1* — basic, *2* — FBCM and *3* — PS) at the CdS-FeS heterophase structure formation stages, where Δ_1 is the CdS/ArchFe surface parameter variation with respect to CdS, Δ_2 is the CdS-FeS surface parameter variation with respect to CdS/ArchFe, Δ_3 is the CdS-FeS surface parameter variation with respect to CdS.

is comparable with the original substrate nonuniformities, enveloping the CdS irregularities, the ArchFe layer smooths the irregularities. This also is indirectly indicative of a nanoscale size of new phases after annealing comparable with the size of original substrate irregularities, this is the case when an insignificant increase in the average value and decrease in dispersion may be expected.

Let's consider additional information that can be acquired from the analysis of AFM images recorded by the FBCM and PS methods. The average FBCM signal is the highest for the hybrid structure surface, and these signals are lower and differ slightly for the original CdS substrate and final CdS-FeS material (Figure 4, a). Visual analysis of Figure 2, a makes it possible to see clear outlines of small

nonuniformities that are absent in Figures 1, *a* and 3, *a*. Therefore they may be associated with the organic coating and its defects. Values of S_q (Figure 4, *b*) measured by the FBCM method decrease in transitions from the first process stage to the next one, thus, providing an additional confirmation of uniform organic layer deposition and uniform distribution of new phases in CdS-FeS after annealing.

Average PS signal variations are most significant in transition from the original surface to the modified one — when ArchFe was deposited, the signal varied by a factor of approximately 8 compared with the original CdS substrate, and decreased by factor of 1.5 after annealing and heterophase structure formation compared with the original substrate, and increased by a factor of approximately 4.4 compared with the hybrid surface (see the table), while the relative variations vary from 32 to 364 % (Figure 4, *a*). Thus, the PS variation is greater by many times than the texture variation because surface viscosity and elasticity have changed. Variations of S_q determined by the PS method decrease from stage to stage (Figure 4, *b*), which once more suggests that the surfaces are even at all process stages.

γ_1 and γ_2 for the FBCM and PS methods are much higher in absolute value, indicating that local areas of these scans are more contrast with respect to the basic AFM images. Moreover, they vary differently during surface modification depending on the signal recording method — in particular, the value of γ_2 for the AFM method shows good agreement with the Gaussian distribution of the final sample (i.e. indicates surface uniformity), but for the FBCM signal, the distribution is „flatter“ and has less pronounced tails, i.e. the FBCM signal distribution consists of closely-spaced Gaussian distributions, which is typical for detecting small surface irregularities.

Thus, it is shown that combination of AFM oscillatory techniques was used to characterize organic, structured Fe coating deposited onto CdS and used for the diluted semimagnetic semiconductor formation process. The PS method may be considered to be the most effective, when formation of a hybrid structure or heterophase surface shall be controlled, or uniformity of the above-mentioned surfaces shall be analyzed not only by morphology, but also by chemical and physical properties.

Funding

The study was partially supported by grant No. 22-22-00194 provided by the Russian Science Foundation, https://rscf.ru/project/22-22-00194/

Conflict of interest

The authors declare no conflict of interest.

References

[1] P.V. Badikova, D.V. Zavyalov, E.S. Sivashova, Technical Physics, 70 (3), 424 (2025). DOI: 10.61011/TP.2025.03.60845.310-24
[2] T.A. Pisarenko, D.A. Tsukanov, V.V. Balashev, A.A. Yakovlev. Technical Physics, 70 (4), 731 (2025). DOI: 10.61011/JTF.2025.04.60013.138-24
[3] A.G. Rokakh, D.I. Bilenko, M.I. Shishkin, A.A. Skaptsov, S.B. Venig, M.D. Matasov. Semiconductors, 48 (12), 1562 (2014). DOI: 10.1134/S1063782614120197 http://journals.ioffe.ru/articles/41150
[4] N.K. Morozova, I.I. Abbasov. Semiconductors, **56** (5), 333 (2022). DOI: 10.21883/SC.2022.05.53427.9793
[5] V.M. Salmanov, A.G. Guseinov, M.A. Jafarov, R.M. Mamedov, T.A. Mamedova. Optics and Spectroscopy, **130** (10), 1308 (2022). DOI 10.21883/eos.2022.10.54868.2983-22
[6] S.V. Stetsyura, P.G. Kharitonova, I.V. Malyar. Applied Physics, **5**, 66 (2020) http://applphys.orion-ir.ru/appl-20/20-5/PF-20-5-66.pdf
[7] S.V. Stetsyura, P.G. Kharitonova, A.V. Kozlowski. Izv. Sarat. Univ. Nov. Ser. Ser.: Fizika, **25** (1), 93 (2025). (in Russian). DOI: 10.18500/1817-3020-2025-25-1-93-105
[8] T. Tohidi, N. Yousefpour Novini, K. Jamshidi-Ghaleh. Optical Mater., **151**, 115394 (2024). DOI: 10.1016/j.optmat.2024.115394
[9] B. Lohitha, S. Thanikaikarasan, S. Roji Marjorie. Materials Today: Proceedings, **33** (7), 3068 (2020). DOI: 10.1016/j.matpr.2020.03.513
[10] K. Kaur, G.S. Lotey, N.K. Verma. J. Mater. Sci.: Mater. Electron., **25**, 2605 (2014). DOI: 10.1007/s10854-014-1918-y
[11] S.V. Stetsyura, P.G. Kharitonova, E.G. Glukhovskoy. St. Petersburg State Polytechnical University J. Phys. and Math., **15** (3.3), 250 (2022). DOI: 10.18721/JPM.153.349
[12] P.G. Kharitonova, E.G. Glukhovskoy, A.V. Kozlowski, S.V. Stetsyura. Semiconductors, **57** (7), 510 (2023). DOI: 10.61011/SC.2023.07.57411.4912C
[13] S.V. Stetsyura, P.G. Kharitonova. St. Petersburg State Polytechnical University J. Phys. and Math., **16** (1.2), 236 (2023). DOI: 10.18721/JPM.161.236
[14] T.N. Shchukovskaya, A.Yu. Goncharova, S.A. Bugorkova, P.S. Erokhin, O.M. Kudryavtseva. Journal of microbiology, epidemiology and immunobiology, **98** (3), 298 (2021) DOI: 10.36233/0372-9311-93
[15] B. Basnar, G. Friedbacher, H. Brunner, T. Vallant, U. Mayer, H. Hoffmann. Appl. Surf. Sci., **171**, 213 (2001). DOI: 10.1016/S0169-4332(00)00761-3
[16] N.A. Davletkildeev, A.V. Kozinskaya, V.F. Azarov, A.V. Glotov. Vestn. Omskogo un-ta, **62**, 114 (2011). (in Russian). https://herald-journal.omsu.ru/issues/134/6417.php
[17] U. Maver, T. Velnar, M. Gaberscek, O. Planinsek, M Finsgar. TrAC Trends in Anal. Chem., **80**, 96 (2016). DOI: 10.1016/j.trac.2016.03.014

Translated by E.Ilinskaya